Eur. Phys. J. A (2018) **54**: 138
DOI 10.1140/epja/i2018-12577-3

THE EUROPEAN PHYSICAL JOURNAL A

Regular Article – Experimental Physics

The partial widths of the 16.1 MeV 2^+ resonance in ^{12}C

Michael Munch[a] and Hans Otto Uldall Fynbo

Department of Physics and Astronomy, Aarhus University, Ny Munkegade 120, 8000 Aarhus C, Aarhus, Denmark

Received: 30 May 2018 / Revised: 22 July 2018
Published online: 27 August 2018

Communicated by P. Woods

Abstract. The 16.1 MeV 2^+ resonance in ^{12}C situated slightly above the proton threshold can decay by proton, α, and γ emission. The partial width for proton emission cannot be directly measured due to the low proton energy and the small branching ratio. Instead it must be indirectly derived from other observables. However, due to several inconsistent data the derived partial width varies by almost a factor 2 depending on the data used. Here we trace the majority of this inconsistency to different measurements of the (p,α) cross sections. We have remeasured this cross section using modern large area silicon strip detectors allowing to measure all final state particles, which circumvents a normalization issue affecting some of the previous measurements. Based on this we determine $\Gamma_p = 21.0(13)$ eV. We discuss the implications for other observables related to the 16.1 MeV 2^+ resonance and for isospin symmetry in the $A = 12$ system. In addition, we conclude that the dataset currently used for the NACRE and NACRE II evaluation of the ^{11}B$(p,3\alpha)$ reaction should be scaled by a factor of 2/3. This impacts the reaction rate accordingly.

1 Introduction

Situated just above the proton threshold, the 16.1 MeV 2^+ state in ^{12}C has been the subject of numerous studies [1–14] with the most recent compilation published in ref. [15] and a detailed review of the decay properties of the 16.1 MeV state given in ref. [12]. The state has primarily been investigated with the $p + {}^{11}$B reaction and it is known to decay via proton, α particle and γ ray emission as illustrated in fig. 1.

In one of the first applications of the concept of isospin, the narrow width of only roughly 5 keV of this state situated higher than 8 MeV in the 3α continuum was explained by Oppenheimer and Serber to be due to its $T = 1$ nature [16]. Hence, its dominating α-decay mode is only possible due to admixtures of $T = 0$ in the state.

In the narrow resonance limit the measured cross sections, σ_{px}, can be related to the partial widths, Γ_x, of the resonance

$$\sigma_{px} = 4\pi\lambda^2\omega\frac{\Gamma_p\Gamma_x}{\Gamma^2}\,, \tag{1}$$

where $\omega = \frac{2J+1}{(2j_0+1)(2j_1+1)}$ with J the resonance spin and j_i the spin of the beam and target. $\lambda = \hbar/E$ is the reduced de Broglie wavelength with the center of mass energy, E. Γ_p has a key role in this relation, but due to the low proton energy and the fact that $\Gamma_p/\Gamma \ll 1$, it is not feasible to measure it directly. Instead, Γ_p must be inferred from measurements of both Γ_x and σ_{px}. This extraction was performed in both refs. [12,15], however, the resulting proton widths differ by almost a factor of 2.

The decay properties of $T = 1$ isobaric analog states in the $A = 12$ system was analysed by Monahan *et al.* [17]. This analysis was based on a comparison of the proton widths in ^{12}C with the neutron spectroscopic factors in ^{12}B deduced from the ^{11}B$(d,p)^{12}$B reaction. Good agreement was found for most states with the notable exception of the 16.1 Mev state. The discrepancy was traced to a too large value for the proton width. Recently the ^{11}B$(d,p)^{12}$B reaction was remeasured with a new method which confirmed the spectroscopic factors deduced previously within 25% [18]. The proton width recommended by ref. [15] results in good agreement with this spectroscopic factor, while that of ref. [12] does not. In the following we will summarize the results of previous measurements and attempt to clarify the situation.

γ ray emission predominantly occurs to the ground state (GS), γ_0, and the first excited state, γ_1, in ^{12}C. The cross sections for the (p,γ) reactions were most recently measured by He *et al.* using a thin target for the first time [13]. Here they confirmed the prior cross section measurements [1,4,8,9,14,19,20] yielding a combined result of $\sigma_{p\gamma 0} = 5.1(5)\,\mu$b and $\sigma_{p\gamma 1} = 139(12)\,\mu$b. Thus we consider the values for these cross sections to be reliable. Complementary to these measurements, Friebel *et al.* directly measured $\Gamma_{\gamma 0} = 0.346(41)$ eV using inelastically scattered electrons [10], while Cecil *et al.* have mea-

[a] e-mail: mm@phys.au.dk

Table 1. Prior measurements of the (p, α) channel.

Measurement	$\sigma_{\alpha,0}$ [mb]	$\sigma_{\alpha,1}$ [mb]	σ_α [mb]	$\sigma_{\alpha,1}/\sigma_{\alpha,0}$	Γ [keV]
Huus *et al.* [1]					~ 5
Beckman *et al.* [2]	$0.2 \pm 30\%$[a]	$10 \pm 30\%$[a]			
Segel *et al.* [3]				22(3)	
Anderson *et al.* [4]			41(3)[b]		6.7
Davidson *et al.* [5]			54(6)		$5.2^{+0.5}_{-0.3}$
Becker *et al.* [6]	$2.12 \pm 5\%$	$69.6 \pm 5\%$[c]		33(2)	5.3(2)
Laursen *et al.* [7]				19.6(19)	

[a] The authors note that the α particles were "barely detectable" [2]. This result will be disregarded.
[b] Assuming infinite target thickness and using the combined Γ of refs. [4,6] this should be rescaled from 38.5(32) mb.
[c] The authors note that their model did *not* reproduce the α_1 data.

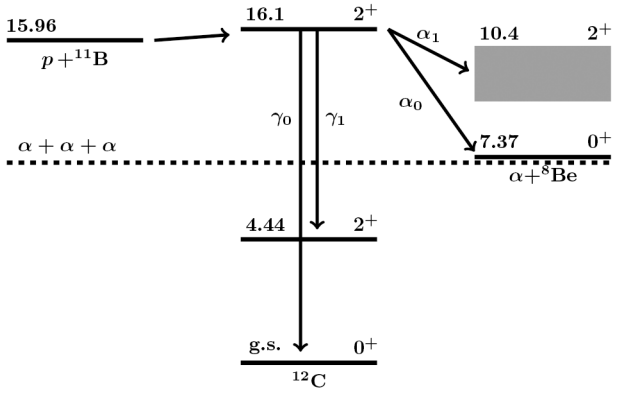

Fig. 1. Illustration of the reaction scheme. The 16.11 MeV 2^+ state ^{12}C is populated with the $p+^{11}$B reaction. The state can either decay via γ, α or proton emission. Energies and spin assignments are taken from ref. [15]. Energies are in MeV.

sured the relative yield of γ rays and charged particles; $\Gamma_{\gamma 0}/\Gamma_\alpha = 6.7(3) \times 10^{-5}$ and $\Gamma_{\gamma 1}/\Gamma_\alpha = 2.0(3) \times 10^{-3}$ [8].

The current understanding of the α particle decay mechanism is a sequential decay proceeding either through the ^{8}Be GS, α_0, or the first excited state, α_1 [7]. The results of prior investigations of the (p, α) channel are listed in table 1. There are multiple consistent measurements for the resonance width and combining the results from refs. [5,6] yields 5.28(18) keV. As these are extracted from a simple resonance scan we consider them reliable. Two out of three measurements of the α_1/α_0 branching ratio are consistent and, as the measurement by Laursen *et al.* was done with coincident detection of multiple final state particles, we also consider the branching ratio reliable. The measured total cross sections for (p, α) generally show poor agreement. However, considering the (p, α_0) reaction yields a distinct high energy peak we expect the $\sigma_{p,\alpha 0}$ measurement by Becker *et al.* to be accurate [6].

By combining the various measurements for the α- and γ channels with eq. (1) and approximating $\Gamma \approx \Gamma_\alpha$ it is possible to derive several independent values for Γ_p. These are listed in table 2. Interestingly, the values seem to cluster into two groups, with the measurements for (p, α) split across the groups.

Table 2. Calculated values for Γ_p. The values are calculated using eq. (1) with the quantities listed in the left column. In all cases $\Gamma = 5.28(18)$ keV was also used. The approximation $\Gamma_\alpha \approx \Gamma$ was applied.

Method	Γ_p [eV]
$\sigma_{p\alpha}$ [4]	20(2)
$\sigma_{p\alpha 0}$ [6] + $\Gamma_{\alpha 1}/\Gamma_{a0}$ [3,7]	22(3)
$\sigma_{p\alpha}$ [5]	26(3)
$\sigma_{p\alpha}$ [6]	34(6)
$\sigma_{p\gamma 1}$ [13] + $\Gamma_{\gamma 1}/\Gamma_a$ [8]	35(3)
$\sigma_{p\gamma 0}$ [13] + $\Gamma_{\gamma 0}/\Gamma_a$ [8]	37(6)
$\sigma_{p\gamma 0}$ [13] + $\Gamma_{\gamma 0}$ [10]	38(6)

All of the cross section measurements of the (p, α) channel were performed with a small energy sensitive detector placed at various angles. The measured energy spectrum was then extrapolated to 0 and integrated. References [4,5] performed a linear extrapolation, while ref. [6] used a sequential decay model. Although Becker *et al.* note their model performed poorly at this resonance, it does *not* explain the discrepancy between the measurements. The key difference is the choice of normalization for the α_1 measurement where Becker *et al.* argue that their detector has either detected the primary alpha particle α_1 or the two secondary α particles from the subsequent ^{8}Be break-up. Thus, they divide their count number by 2. On the contrary, refs. [4,5] argue they observe one out three final state α particles and divide by a factor of 3. The probability for detecting both secondary α particles in a single detector was discussed theoretically by Wheeler in 1941 [21]. The probability depends on the opening angle between the secondary α particles and the aperture of the detector. The opening angle in turn depends on the energy of the ^{8}Be system with respect to the α threshold. This is small for the ^{8}Be GS but quite significant for the first excited state. Based on information provided in ref. [6] we have estimated their maximum detector aperture to be of

the order of 3°. In this case the probability for a double hit is minuscule —even for the α_0 channel. Thus, the α_1 results by Becker *et al.* should most likely be scaled by a factor of 2/3 making it consistent with the other two measurements. The astrophysical NACRE evaluation [22] explicitly mentions this discussion in their $^{11}\mathrm{B}(p,3\alpha)$ evaluation, where they use the dataset of Becker *et al.* for its recommended value while using the dataset of refs. [5,23] as a lower limit. The updated evaluation NACRE II [24] is less cautious and relies solely on Becker *et al.*

The magnitude of the $\sigma_{p\alpha}$ cross section has implications beyond nuclear structure. For example the $^{11}\mathrm{B}(p,3\alpha)$ reaction is a candidate for a fusion reaction generating energy without neutrons in the final state, see *e.g.* [25]. The rate of this reaction at the energies relevant for a fusion reactor is mainly determined by the 16.1 MeV 2^+ and the higher lying 16.6 MeV 2^- resonances. The proton width is related to the $^{11}\mathrm{B}(d,p)^{12}\mathrm{B}$ reaction by isospin symmetry. In turn, that reaction is used to deduce the $^{11}\mathrm{B}(n,\gamma)^{12}\mathrm{B}$ reaction cross section, which may play a role in the astrophysical r-process [18].

The object of this paper is to remeasure $\sigma_{p\alpha}$ in order to clarify the situation. The measurement will circumvent the normalization ambiguity by observing all three particles in coincidence using an array of large area segmented silicon detectors. In this paper we will only address the cross section of the 16.1 MeV state, but the discussion on normalization applies universally to all measurements of this reaction, where the cross section is inferred from a single detector.

2 Experiment

A thin foil of $^{11}\mathrm{B}$, oriented 45° with respect to the beam axis, was bombarded with a beam of H_3^+ molecules. A resonance scan was conducted between 460 and 600 keV and afterwards data was collected for 30 hours at 525 keV. The beam was provided by the 5 MV Van de Graaff accelerator at Aarhus University and the beam spot was defined by a pair of 1×1 mm vertical and horizontal slits. The energy of the accelerator was prior to the experiment energy calibrated using narrow (p,α) resonances in $^{27}\mathrm{Al}$ and the energy resolution was found to be better than a few keV for single charged beams. It should be noted that the energy stability is trifold improved for H_3^+.

Upon impact with the target foil the H_3^+ molecules will break up and additional electron stripping, neutralization and scattering might occur. This affected the integrated beam current, which was measured with a Faraday cup 1 m downstream of the target. The combined effect of this can be determined from the ratio of the observed current both with and without a target foil in the beam. At the beginning of the experiment the effective charge state was determined to be 1.72(5)e. However, this ratio was observed to change during the experiment. We attribute this to carbon build-up on the target. The change in charge state was $4.33(4) \times 10^{-3}\,\mu\mathrm{C}^{-1}$. Correcting for this, a total of 61(6) μC was collected on the resonance.

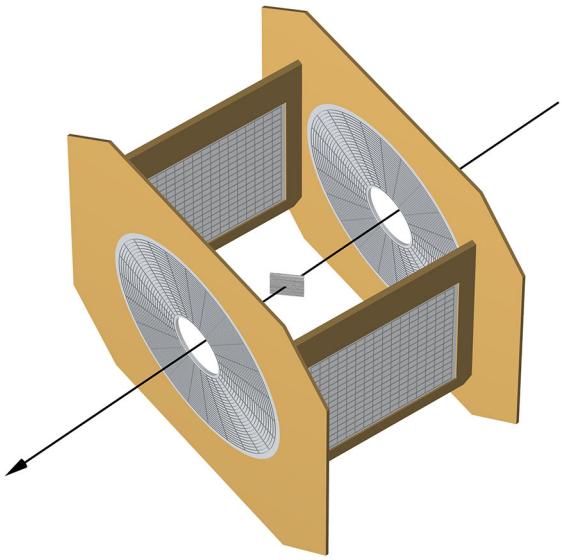

Fig. 2. Schematic drawing of the experimental setup. An arrow indicates the incoming proton beam. The enriched boron target was oriented 45° with respect to the beam axis. Two quadratic and two annular double sided silicon strip detector were used to detect outgoing particles. Front and back segmentation is shown simultaneously for clarity.

The target was produced at Aarhus University by evaporation of 99% enriched $^{11}\mathrm{B}$ onto a 4 $\mu\mathrm{g/cm}^2$ carbon backing. The thickness was measured by bombarding the target with 2 MeV α particles and the boron layer either facing towards or away from the beam. Assuming a two layer target the boron thickness can be inferred from the energy shift of particles scattered off the carbon layer using the procedure of ref. [26], but including a correction for the changed stopping power of the scattered particle.

$$t = \frac{\delta E}{K(\theta)S(E_b) + S(K(\theta)E_b)/\cos\theta}\,, \tag{2}$$

where E_b the beam energy, S the stopping power, δE the energy difference and K is the kinematic factor for the laboraty scattering angle, θ, defined as

$$K = \frac{m_b\cos\theta + \sqrt{m_t^2 - m_b^2\sin^2\theta}}{m_b + m_t}\,, \tag{3}$$

where m_t, m_b is the mass of the target and beam ion respectively. The cosine factor in eq. (2) corrects for the increased path length for the scattered particle. The result is 39(3) $\mu\mathrm{g/cm}^2$. The energy loss for a 525/3 keV proton through this target is 23(2) keV according to the SRIM stopping power tables [27].

Charged particles were observed with an array of double sided silicon strip detectors (DSSD) giving a simultaneous measurement of position and energy. A sketch of the array can be seen on fig. 2. The array consisted of two annular DSSD (S3 from Micron Semiconductors) placed 36 mm up- and downstream of the target; covering the angles between 140 and 165° and 23 and 36° respectively. Each annular ring is approximately 1 mm wide with

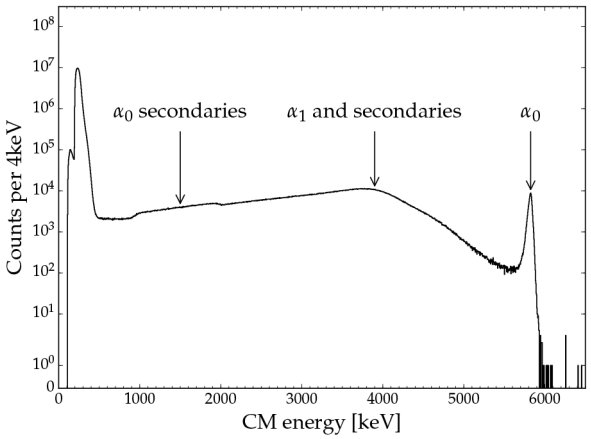

Fig. 3. Full CM energy spectrum without any cuts. The high energy peak corresponds to the primary α particle, α_0.

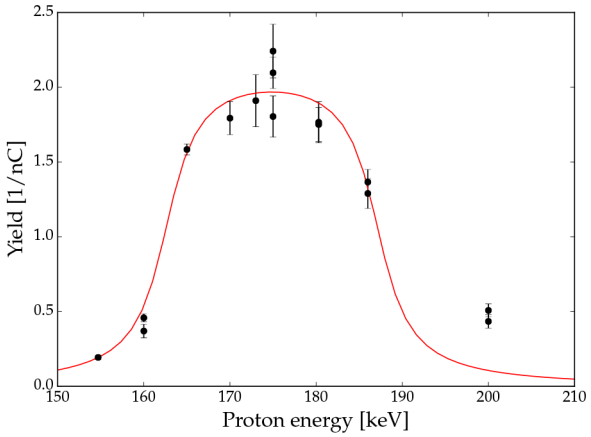

Fig. 4. Scan of the 162 keV resonance. The individual data points corresponds to the α_0 yield, while the solid curve is the best fit to eq. (4).

an approximate 2° resolution in polar angle. Additionally, two quadratic DSSDs (W1 from Micron Semiconductors) were placed 40 mm from the target center at an angle of 90° with respect to the beam axis. These covered angles between 60° and 120°. All pixels are 3 × 3 mm with an approximate angular resolution of 4°.

3 Analysis

The analysis is structured in the following way. First a resonance scan is shown for the α_0 channel. This is followed by an extraction of the α_0 angular distribution and cross section from the multiplicity 1 data. Building upon this follows the analysis of the triple events, *i.e.* events with exactly three alpha particles and afterwards a brief discussion of how the detection efficiencies for the α_0 and α_1 channel have been determined.

3.1 Singles analysis

Assuming all ejectiles to be α particles the center-of-mass (CM) energy can be determined from the detected position and energy. The full spectrum, without any cuts, is shown in fig. 3. The spectrum shows a clear peak at 5.8 MeV, which is consistent with a sequential decay of the 16.1 MeV state via the GS of ^{8}Be. The α particle giving rise to this peak will be referred to as the primary α particle. Below the peak is a broad asymmetric distribution, which consists of secondary α particles and α particles from the break-up via the first excited state of ^{8}Be. At low energy the proton peak is visible. It is double peaked since energy loss corrections are applied as if it was an α particle.

The primary α particle is selected by requiring $E_{\mathrm{CM}} > 5.65$ MeV. Figure 4 shows the α_0 yield as a function of proton energy. The yield is clearly resonant and peaks at ~ 175 keV. The curve shown in the figure is the best fit to the thick target yield for a Breit-Wigner shaped resonance [28]

$$Y = \left[\tan^{-1}\frac{E_p - E_r}{\Gamma_{\mathrm{lab}}/2} - \tan^{-1}\frac{E_p - E_r - \Delta E}{\Gamma_{\mathrm{lab}}/2}\right] \times \frac{\Gamma_{\mathrm{lab}}\,\sigma_{\mathrm{BW}}(E = E_r)}{2\epsilon}\eta, \tag{4}$$

where Γ_{lab} is the resonance width in the lab system, E_p is the beam energy, E_r the resonance energy, ΔE the energy loss through the target, η the detection efficiency, σ_{BW} the resonant Breit-Wigner cross section and $\epsilon = \frac{1}{N}\frac{\mathrm{d}E}{\mathrm{d}x}$, where N is the number density of target nuclei and $\frac{\mathrm{d}E}{\mathrm{d}x}$ the stopping power. Using the factor outside the parenthesis as a arbitrary scaling factor, the best fit was achieved with $\Delta E = 24.5(9)$ keV, $E_r = 162.6(5)$ keV and Γ_{lab} fixed to $12/11 \cdot 5.28$ keV. The target thickness is consistent with the result obtained from α-scattering and the resonance energy fits with the recommended literature value [20].

The α_0 angular distribution relative to the beam axis was extracted for the long runs at $E_p = 175$ keV. The angular distribution, corrected for solid angle, can be seen in fig. 5. The solid line shows the best fit to the lowest five Legendre polynomials.

$$W(\theta) = A\left[1 + \sum_{i=1}^{4} a_i P_i(\cos\theta)\right]. \tag{5}$$

The coefficients providing the best fit are $a_1 = -0.358(7)$, $a_2 = 0.249(2)$, $a_3 = -0.106(11)$, $a_4 = -9(20) \times 10^{-3}$ and $A = 4.253(17) \times 10^4\,\mathrm{sr}^{-1}$. The lower panel of the figure shows the fit rescaled, $W(90°) = 1$, along with the data from refs. [5,6], which have been rescaled to coincide with the fit at 90°. Good agreement is observed with ref. [5] while the symmetric behavior seen by ref. [6] cannot be reproduced.

The total number of counts is found by integration of eq. (5), *i.e.* $4\pi A$. This can be related to the resonant Breit-Wigner cross section using eq. (4)

$$\sigma_{p\alpha,0} = 2.1(2)\,\mathrm{mb}. \tag{6}$$

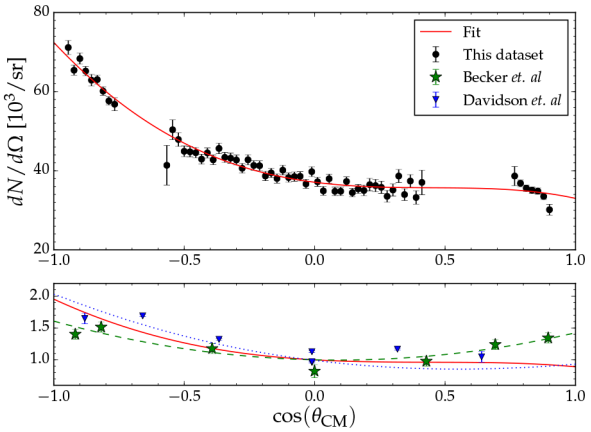

Fig. 5. Angular distribution of this dataset corrected for solid angle along with the best fit to eq. (5). The datasets of refs. [5,6] have been rescaled to coincide with the fit at 90°.

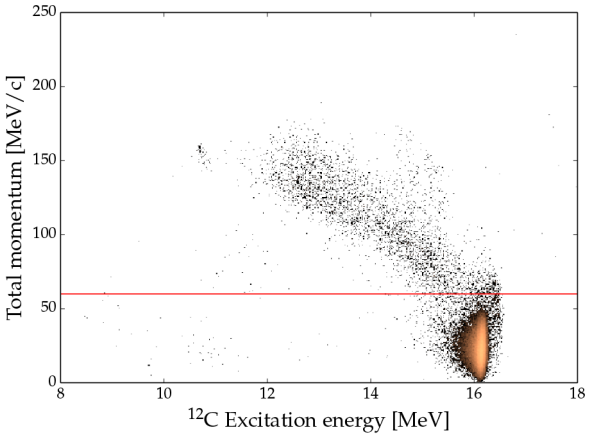

Fig. 6. Total momentum of the three particles in the CM *vs.* the calculated excitation energy of ^{12}C. The red line corresponds to the cut placed at 60 MeV/c.

The main uncertainty is the variation in the effective charge state.

3.2 Extraction of triple events

The end goal of this analysis step is to extract tuples of particles consistent with a decay of the 16.1 MeV state in ^{12}C into three α particles. It applies the methods described in ref. [29].

The first and simplest requirement is that at least three particles must be detected in an event. This massively reduces the data, since the majority of events consist of elastically scattered protons. Furthermore, it is required that all three particles are detected within 30 ns of each other. This reduces the background from random coincidences with protons significantly while $> 99\%$ of good events survive. Additionally, it is required that the sum of CM angles between the CM position vectors must be larger than 350°. All particles surviving these cuts are assumed to be α particles. From the detected energy and position it is possible to calculate the four momentum of each particle. From these, one can calculate the total momentum in the CM and the ^{12}C excitation energy. This is shown in fig. 6, which has a distinct peak at 16.1 MeV. Interestingly, weak peaks are visible at low total momentum and excitation energy lower than 16.1 MeV. These correspond to γ transitions in ^{12}C as observed in ref. [12]. Projecting the individual energy of the high momentum events it is clear that these correspond to events with one proton and two α particles. Hence, all events with $p_{\mathrm{CM}} > 60$ MeV/c are removed.

The classification of whether a tuple corresponds to a decay via the GS or first excited state, can be done based on whether the CM energy of the most energetic particle lies within the high energy peak in fig. 3. This is the same cut used in sect. 3.1. With this classification the count numbers for the two channels are

$$N_0 = 3.318(18) \times 10^4 \quad (7)$$

$$N_1 = 4.33(2) \times 10^4, \quad (8)$$

where the uncertainties are due to counting statistics.

3.3 Detection efficiency of the α_0 channel

In order to relate the observed number of counts to a yield it is necessary to determine the detection efficiency. For the ground state this is simple. A beam with a 1×1 mm profile was generated and propagated to a random depth in the target. Here α_0 was generated and emitted according to the observed angular distribution in fig. 3. The secondary particles were ejected isotropically according to conservation of angular momentum. These particles were propagated out of the target and into the detectors. Energy loss was taken into account using the SRIM energy loss tables [27]. The output of the simulation had a structure which was identical to the data and was thus subjected to the same analysis. From the survival ratio an acceptance was determined

$$\eta_0 = 7.1(3)\%. \quad (9)$$

Correcting for the efficiency gives a cross section of

$$\sigma_{p\alpha,0} = 2.0(2)\,\mathrm{mb}, \quad (10)$$

which is consistent with the singles analysis.

3.4 Detection efficiency of the α_1 channel

The detection efficiency depends heavily on the ^{8}Be excitation energy as it determines the opening angle between the secondary α particles. Laursen *et al.* found that their sequential decay model fully described their data [7]. Thus, events were generated using this model. Propagation and energy loss was done with the same procedure as described in the previous section. From the survival ratio the acceptance was determined to be

$$\eta_1 = 0.49(5)\%. \quad (11)$$

This yields a cross section to the excited channel of

$$\sigma_{p\alpha,1} = 38(5)\,\mathrm{mb}. \quad (12)$$

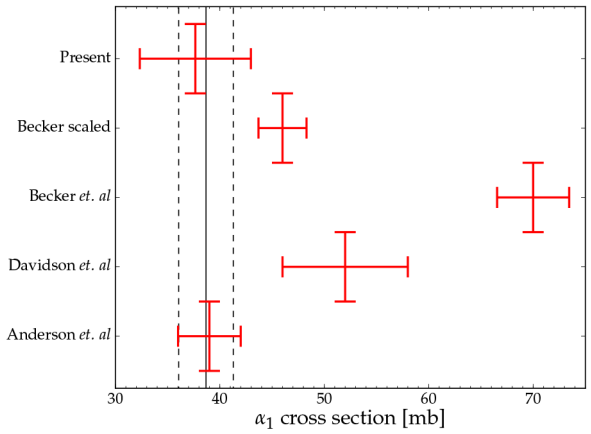

Fig. 7. Comparison of the present α_1 cross section with the measurement of refs. [4–6]. Becker scaled is the data from ref. [6] scaled by 2/3. The full line is the mean recommended value while the dashed lines show the one sigma limit. See text for details.

4 Discussion

Both values determined for the α_0 cross section are consistent with the measurement by Becker *et al.* The weighted cross section is

$$\sigma_{p\alpha,0} = 2.03(14)\,\text{mb}. \tag{13}$$

Comparing the angular distribution in fig. 5 with previous measurements, good agreement is observed for the region around 90 deg. However, while ref. [6] finds the distribution to be nearly symmetric around 90 deg, this conclusion is not supported by the present measurement or ref. [5]. Importantly, the integrated cross section is not very sensitive to the large angle behavior, which explains the good agreement obtained nevertheless.

In order to compare $\sigma_{p\alpha,1}$ between the different measurements, it is computed as $\sigma_{p\alpha,1} = \sigma_{p\alpha} - \sigma_{p\alpha_0}$ for refs. [4, 5]. The result is shown in fig. 7 along with the present α_1 cross section and that of ref. [6]. From the figure the excellent argeement between the present measurement and ref. [4] can be observed. Both values deviate more than 2α from the measurement of ref. [5]. We suspect this is due to an overall normalization problem in ref. [5]. The original measurement by ref. [6] differs significantly from all other measurements, but if rescaled by a factor 2/3, corresponding to the different normalization choice, the data point is in agreement within the errors. However, in light of the systematic problems reported by ref. [6] for the 16.1 MeV resonance the value is not included in the recommended value[1]. Instead the recommended α_1 cross section is based on the results from the present experiment and ref. [4]

$$\sigma_{p\alpha,1} = 39(3)\,\text{mb}. \tag{14}$$

[1] The short-comings of their model at the 16.1 MeV resonance is due to them neglecting interference terms by summing incoherently over different α permutations. The importance of interference was demonstrated in the work of refs. [30, 31].

Similarly the recommended total α cross section is

$$\sigma_{p\alpha} = 41(3)\,\text{mb}. \tag{15}$$

The ratio of the two α channels from the present measurement is 19(3), which is consistent with both previous measurements. Combining all three measurements yields

$$\frac{\sigma_{p\alpha,1}}{\sigma_{p\alpha,0}} = 19.9(14). \tag{16}$$

5 Derived partial widths

Using the present measurement of the (p,α) cross section the partial proton width can be determined using eq. (1)

$$\Gamma_p = 19(3)\,\text{eV}, \tag{17}$$

while using the combined cross section yields

$$\Gamma_p = 19.7(13)\,\text{eV}. \tag{18}$$

Both values are consistent, within the errors, with that of the latest compilation [15], but not with the value favored in the recent review in ref. [12].

Combining this proton width with the results of He *et al.* and Γ, the partial gamma widths can be determined

$$\Gamma_{\gamma 0} = 0.66(9)\,\text{eV} \tag{19}$$
$$\Gamma_{\gamma 1} = 18(2)\,\text{eV}. \tag{20}$$

These values are consistent with the latest compilation [15], but inconsistent with a direct measurement using inelastically scattered electrons, which measured $\Gamma_{\gamma 0} = 0.346(41)$ eV [10]. While direct measurements should generally be favored, in this case there is multiple independent and consistent measurements of the remaining parameters. In order to resolve this discrepancy we suggest that $\Gamma_{\gamma 0}$ is remeasured in a direct manner. The argument in the recent review hinged on this value being correct [12].

Combining the improved total α cross section with the γ cross sections measured by He *et al.* the branching ratio can be determined

$$\frac{\Gamma_{\gamma 0}}{\Gamma_\alpha} = 1.18(13)\times 10^{-5} \tag{21}$$
$$\frac{\Gamma_{\gamma 1}}{\Gamma_\alpha} = 3.2(3)\times 10^{-3}, \tag{22}$$

which is inconsistent with the measurement by Cecil *et al.* Considering the general spread of the measured α cross sections, the most likely explanation for this discrepancy is that Cecil *et al.* have overestimated the α yield.

Using the updated proton width the ratio between the reduced proton and neutron width can be computed. The analysis in ref. [17] was performed with $\Gamma_p = 69$ eV and an updated value can be computed by scaling accordingly

$$\frac{\gamma_n^2}{2\gamma_p^2} = 0.63. \tag{23}$$

This shows a similar degree of isopin symmetry as the other bound states analysed in the $A = 12$ system [17].

6 Conclusion

Using the $p + {}^{11}\mathrm{B}$ reaction, the break-up of the 16.1 MeV state in $^{12}\mathrm{C}$ into three α particles has been studied using an array of large area segmented silicon detectors in close geometry. The decay via the ground state of $^{8}\mathrm{Be}$ has been studied both with detection of single particles and coincident detection of all three α particles. The derived cross sections are internally consistent and the combined result is

$$\sigma_{p\alpha,0} = 2.03(14)\,\mathrm{mb}, \tag{24}$$

which is consistent with the result of ref. [6].

Currently, there exist multiple incompatible measurements of the decay via the first excited state of $^{8}\mathrm{Be}$. This channel was studied using coincident detection of all three α particles. The coincidence acceptance was determined using the decay model of ref. [7] yielding a model dependent cross section

$$\sigma_{p\alpha,1} = 38(5)\,\mathrm{mb}. \tag{25}$$

which is, within the errors, consistent with ref. [4] but not refs. [5,6].

The inconsistency with ref. [6] is due to their claim of having a substantial chance of detecting two out of three particles with a single detector. This was discussed based on ref. [21]. The chance of this is minuscule and hence the entire α_1 dataset of ref. [6] should be rescaled by a factor 2/3. This has a significant impact on the recommended astrophysical reaction rate, as both NACRE [22] and NACRE II [24] have based their recommended values on the dataset provided by ref. [6]. The recommended reaction rate should thus be scaled accordingly. In addition, this also has implications for the expected yield from an aneutronic fusion reactor.

Combining the present measurement of $\sigma_{p\alpha}$ with that of ref. [4] a refined partial proton width of $\Gamma_p = 19.7(13)\,\mathrm{eV}$ was deduced. This in turn, was used to determine the partial gamma widths $\Gamma_{\gamma 0} = 0.68(8)\,\mathrm{eV}$ and $\Gamma_{\gamma 1} = 18(2)\,\mathrm{eV}$, using the combined γ cross sections reported by ref. [13]. The value for $\Gamma_{\gamma 0}$ differs by roughly a factor of 2 from the direct measurement of ref. [10]. Hence, we recommend that $\Gamma_{\gamma 0}$ is remeasured. Based on these results, we can no longer recommend the proton width deduced in ref. [12].

Additionally, improved γ-α branching ratios are derived. These are roughly a factor of 2 larger than the measurements published by ref. [8]. We speculate that this discrepancy is most likely due to ref. [8] having overestimated the α yield.

The recommended value for the proton width can be compared to the spectroscopic factor for the analog state in $^{12}\mathrm{B}$. By using the analysis presented in [17] the ratio of the corresponding reduced widths is 0.63, which shows a similar degree of isopin symmetry as the other bound states analysed in the $A = 12$ system. A modern calculation of the proton width would be highly interesting.

We would like to thank Folmer Lyckegaard for manufacturing the target. We also acknowledge financial support from the European Research Council under ERC starting grant LOBENA, No. 307447.

References

1. T. Huus, R.B. Day, Phys. Rev. **91**, 599 (1953).
2. O. Beckman, T. Huus, Č. Zupančič, Phys. Rev. **91**, 606 (1953).
3. R.E. Segel, M.J. Bina, Phys. Rev. **124**, 814 (1961).
4. B. Anderson, M. Dwarakanath, J. Schweitzer, A. Nero, Nucl. Phys. A **233**, 286 (1974).
5. J.M. Davidson, H.L. Berg, M.M. Lowry, M.R. Dwarakanath, A.J. Sierk, P. Batay-Csorba, Nucl. Phys. Sect. A **315**, 253 (1979).
6. H.W. Becker, C. Rolfs, H.P. Trautvetter, Z. Phys. A At. Nucl. **327**, 341 (1987).
7. K.L. Laursen, H.O.U. Fynbo, O.S. Kirsebom, K.O. Madsbøl, K. Riisager, K.S. Madsbøll, K. Riisager, Eur. Phys. J. A **52**, 271 (2016) arXiv:1604.01244.
8. F. Cecil, D. Ferg, H. Liu, J. Scorby, J. McNeil, P. Kunz, Nucl. Phys. A **539**, 75 (1992).
9. E.G. Adelberger, R.E. Marrs, K.A. Snover, J.E. Bussoletti, Phys. Rev. C **15**, 484 (1977).
10. A. Friebel, P. Manakos, A. Richter, E. Spamer, W. Stock, O. Titze, Nucl. Phys. A **294**, 129 (1978).
11. S. Stave, M. Ahmed, R. France, S. Henshaw, B. Müller, B. Perdue, R. Prior, M. Spraker, H. Weller, Phys. Lett. B **696**, 26 (2011).
12. K.L. Laursen, H.O.U. Fynbo, O.S. Kirsebom, K.S. Madsbøll, K. Riisager, Eur. Phys. J. A **52**, 370 (2016) arXiv:1610.00509.
13. J.J. He, B.L. Jia, S.W. Xu, S.Z. Chen, S.B. Ma, S.Q. Hou, J. Hu, L.Y. Zhang, X.Q. Yu, Phys. Rev. C - Nucl. Phys. **93**, 1 (2016).
14. D.S. Craig, W.G. Gross, R.G. Jarvis, Phys. Rev. **103**, 1414 (1956).
15. J. Kelley, J. Purcell, C. Sheu, Nucl. Phys. A **968**, 71 (2017).
16. J.R. Oppenheimer, R. Serber, Phys. Rev. **53**, 636 (1938).
17. J.E. Monahan, H.T. Fortune, C.M. Vincent, R.E. Segel, Phys. Rev. C **3**, 2192 (1971).
18. H.Y. Lee, J.P. Greene, C.L. Jiang, R.C. Pardo, K.E. Rehm, J.P. Schiffer, A.H. Wuosmaa, N.J. Goodman, J.C. Lighthall, S.T. Marley *et al.*, Phys. Rev. C **81**, 015802 (2010).
19. F. Ajzenberg, T. Lauritsen, Rev. Mod. Phys. **24**, 321 (1952).
20. F. Ajzenberg-Selove, Nucl. Phys. A **506**, 1 (1990).
21. J.A. Wheeler, Phys. Rev. **59**, 27 (1941).
22. C. Angulo, M. Arnould, M. Rayet, P. Descouvemont, D. Baye, C. Leclercq-Willain, A. Coc, S. Barhoumi, P. Aguer, C. Rolfs *et al.*, Nucl. Phys. A **656**, 3 (1999).
23. R.E. Segel, S.S. Hanna, R.G. Allas, Phys. Rev. **139**, B818 (1965).

24. Y. Xu, K. Takahashi, S. Goriely, M. Arnould, M. Ohta, H. Utsunomiya, Nucl. Phys. A **918**, 61 (2013).
25. D. Moreau, Nucl. Fusion **17**, 13 (1977).
26. M. Chiari, L. Giuntini, P. Mandò, N. Taccetti, Nucl. Instrum. Methods Phys. Res. Sect. B **184**, 309 (2001).
27. J.F. Ziegler, M.D. Ziegler, J.P. Biersack, Nucl. Instrum. Methods Phys. Res. B **268**, 1818 (2010).
28. W.A. Fowler, C.C. Lauritsen, T. Lauritsen, Rev. Mod. Phys. **20**, 236 (1948).
29. M. Alcorta, O. Kirsebom, M. Borge, H. Fynbo, K. Riisager, O. Tengblad, Nucl. Instrum. Methods Phys. Res. Sect. A **605**, 318 (2009).
30. G.C. Phillips, Rev. Mod. Phys. **37**, 409 (1965).
31. K. Schäfer, Nucl. Phys. A **140**, 9 (1970).